Heliyon 10 (2024) e32689

Contents lists available at ScienceDirect

Heliyon

journal homepage: www.cell.com/heliyon

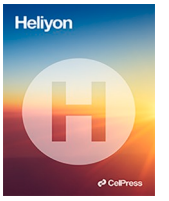

Research article

Intravenous application of human umbilical cord mesenchymal stem cells alleviate neuropathic pain by suppressing microglia activation in rats

Xiaodong Xu [a,b,1], Hui Chen [c,1], Yubei Qiu [d], Ye Chen [a,b], Junle Liu [e], Bangwei Zeng [f], Lei Lin [a], Xinyan Lin [g], Leisheng Zhang [h,i,**], Liangcheng Zhang [a,*]

[a] *Department of Anesthesiology, Fujian Medical University Union Hospital, Fuzhou, 350000, China*
[b] *The Graduate School of Fujian Medical University, Fuzhou, 350000, China*
[c] *Department of Anesthesiology, Zhongshan Hospital (Xiamen), Fudan University, Xiamen, 361015, China*
[d] *School and Hospital of Stomatology, Fujian Medical University, Fuzhou, 350002, China*
[e] *Department of Anesthesiology, Xiamen Third Hospital, Xiamen, 361100, China*
[f] *Administration Department of Nosocomial Infection, Fujian Medical University Union Hospital, Fuzhou, 350000, China*
[g] *Xiamen Public Security Bureau, Xiamen, 361104, China*
[h] *National Health Commission (NHC) Key Laboratory of Diagnosis and Therapy of Gastrointestinal Tumor, Gansu Provincial Hospital, Lanzhou, 730000, China*
[i] *Ji'nan Key Laboratory of Medical Cell Bioengineering, Science and Technology Innovation Center, The Fourth People's Hospital of Jinan, The Teaching Hospital of Shandong First Medical University, Jinan, 250031, China*

ARTICLE INFO

Keywords:
Chronic constriction injury
Neuropathic pain
HUC-MSCs
Microglia activation
Intravenous administration

ABSTRACT

Objective: Neuropathic pain has been considered as one of the most serious chronic pain subtypes and causes intolerable suffering to patients physically and mentally. This study aimed to verify the analgesic effect of intravenous administration of human umbilical cord mesenchymal stem cells (HUC-MSCs) upon rats with chronic constriction injury (CCI)-induced neuropathic pain and the concomitant mechanism via modulating microglia.

Methods: 30 male SD rats were randomized divided into three groups (n = 10 per group): Sham + Saline group (S&S group), CCI + Saline group (C&S group) and CCI + HUC-MSCs group (C&U group). Rats were injected with either saline or HUC-MSCs via the caudal vein on the 7th day after modelling. The paw mechanical withdrawal threshold (PMWT) and thermal withdrawal latency (TWL) of the ligation side were measured before (day 0) and after (day 1, 3, 5, 7, 9, 11, 13, and 15) modelling. On day 15 after modelling, western-blotting and immunofluorescent staining were used to assess the expressive abundance of Iba-1 (a typical biomarker of activated microglia) in the ligation side of the spinal cord dorsal horn, and ultrastructural changes of the ligation of sciatic nerve were evaluated by transmission electron microscope (TEM).

Results: Compared with the S&S group, PMWT and TWL in the C&S group were significantly decreased on day 5 and then persisted to day 15 after modelling (C&S vs S&S, $P < 0.05$), while a significant amelioration of mechanical hyperalgesia (day 13, day 15) and thermal allodynia (day 9, day 11, day 15) was observed in the C&U group (C&U vs C&S, $P < 0.05$). Meanwhile, the

* Corresponding author.
** Corresponding author. National Health Commission (NHC) Key Laboratory of Diagnosis and Therapy of Gastrointestinal Tumor, Gansu Provincial Hospital, Lanzhou, 730000, China.
E-mail addresses: leisheng_zhang@163.com (L. Zhang), zhanglc6@163.com (L. Zhang).
[1] Co-first authors contributed equally to this work.

https://doi.org/10.1016/j.heliyon.2024.e32689
Received 2 March 2023; Received in revised form 23 May 2024; Accepted 6 June 2024
Available online 13 June 2024

expression of Iba-1 was significantly suppressed by systemic infusion of HUC-MSCs in the C&U group according to western-blotting and immunofluorescent staining analyses ($P < 0.05$). With the aid of TEM detection, we intuitively noticed the efficacious reconstruction of the laminate structure of the sciatic nerve ligation, elimination of mitochondrial swelling, and formation of new myelination were noted on day 15 after modelling in the C&U group.
Conclusions: Overall, intravenous administration of HUC-MSCs systemically revealed an ameliorative effect upon CCI-induced neuropathic pain in SD rats by inhibiting microglia activation in the dorsal horn of the impaired spinal cord and alleviating sciatic nerve injury. Our findings supply new references for the further development of HUC-MSCs-based cytotherapy for neuropathic pain administration.

1. Introduction

Neuropathic pain (NP) is a chronic pain condition induced by a disease or damage to the somatosensory nervous system [1,2], and the major clinical manifestations of which include spontaneous pain, hyperalgesia and tactile pain. Despite the tremendous advances in traditional medicine for NP diagnosis and treatment such as drug therapy and physical therapy, patient outcomes remain ineffective, with adverse effects largely attributed to the deficiency of pathogenesis [3]. Among them, microglia in the central nervous system are initially regarded as a class of macrophages, which only respond to damage and have been found to play a more critical role in neuronal signaling [4] as well as the formation and maintenance of neuropathic pain [5,6]. However, the detailed role of microglia in mediating NP and their potential feasibility as a therapeutic target remains unclear. Taken together, there is an urgent need to explore the microglia-associated pathogenesis for the further development of novel therapeutic regimens for managing the intractable NP. Mesenchymal stem/stromal cells (MSCs), also known as medicinal signaling cells, are a heterogeneous and multipotent cell population with unique properties of bidirectional immunomodulation and hematopoietic-supporting effects [7–9]. They are involved in neuroprotection, nerve regeneration and neuroplasticity, and have been used in the treatment of neuroinflammatory diseases [10]. Of the

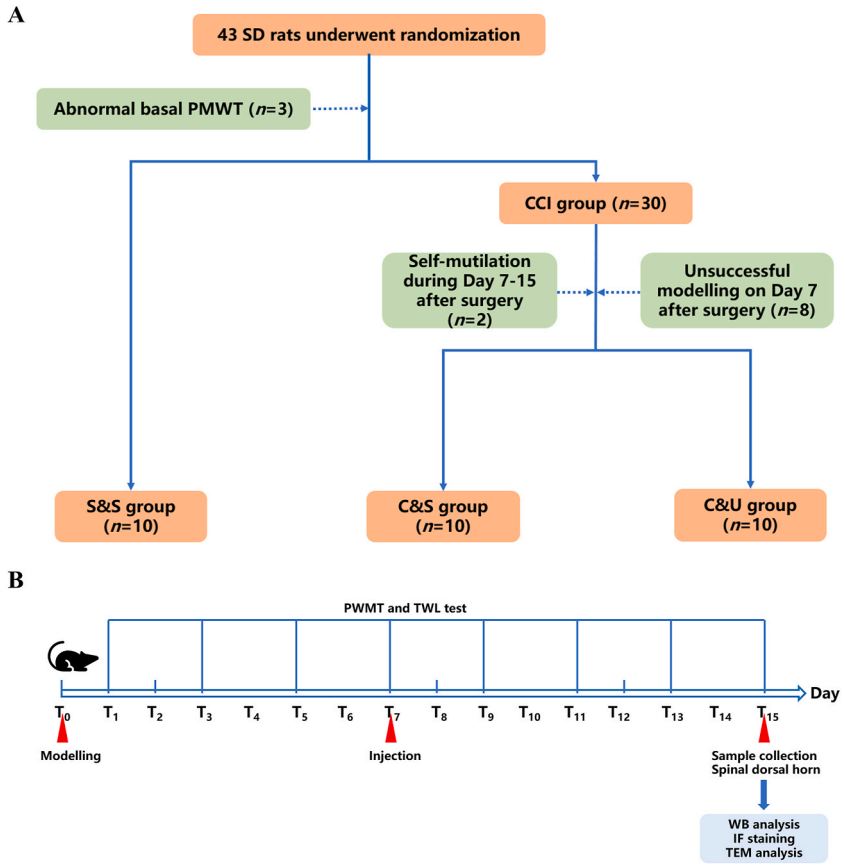

Fig. 1. Schematic diagram of experimental grouping and design flow. A: Schematic diagram of the random allocation and modelling process of 43 SD rats, with 10 rats in each group in the end. B: Flowchart of the pain threshold measurement, injection time, and sample collection for experiments after the modelling, PMWT: Paw Mechanical Withdrawal Threshold, TWL: Thermal Withdrawal Latency.

reported MSCs with diverse origins, HUC-MSCs are gaining increasing favor in the field of peripheral neuropathic pain treatment and research, primarily due to their more robust *in vitro* proliferation, lower immunogenicity, stronger anti-inflammatory ability, and higher tissue survival ability [11–13].

Currently, both single and multiple intrathecal transplantation of HUC-MSCs have been reported as the primary therapeutic approaches, which can alleviate neuropathic pain by inhibiting spinal microglial cell activation [14–16]. Indeed, intrathecal administration with high drug utilization provides a more direct targeting of the sensitized central sites. However, this route of administration is accompanied by inherent risks and drawbacks such as heightened procedural complexities and susceptibility to infections [17]. To date, intravenous injection remains the most commonly used, convenient, and easily applicable method in clinical practice. However, the therapeutic effect of MSCs via intravenous injection might be affected by the potentially depositing in lung [18,19], yet the limited evidence upon peripheral neuropathic pain treatment was inconsistent [20,21]. Therefore, further investigations are imperative to clarify the efficacy and the concomitant underlying mechanisms of MSC administration via intravenous intervention.

In this study, we took advantage of the CCI-induced SD rat model to verify the therapeutic effect and the underlying mechanism of HUC-MSCs on neuropathic pain via intravenous infusion. Our findings provided new references for further illuminating the feasibility of neuropathic pain treatment by systemic HUC-MSC infusion in clinical practice.

2. Materials and methods

2.1. HUC-MSCs culture

HUC-MSCs (passage 3–6) were purchased from Health-Biotech Stem Cell Research Institute Co., Ltd. (Tianjin, China), and cultured in DMEM-F12 basal medium (Gibco, Montana, USA) supplemented with 10 % fetal bovine serum (FBS) (Gibco), 1 % L-glutamine (Gibco), 1 % NEAA (Gibco), 4 ng/ml bFGF (Peprotech, New Jersey, USA), and 4 ng/ml EGF (Peprotech), as we recently reported with several modifications [22,23].

2.2. Animals

As shown in Fig. 1, a total of 43 male Sprague–Dawley (SD) rats (6–8 weeks of age, 120–200 g in body weight) were purchased from Shanghai Slaccas Laboratory Animal Co. Ltd. (Shanghai, China). All rats were housed at the Laboratory Animal Center of Fujian Medical University with controlled room temperature (24 ± 2 °C), relative humidity (60 ± 5 %) and a 12 h light-dark cycle. The rats were allowed access to food and water ad libitum and handled for 7 days to familiarize them with the experimental environment and procedure. SD rats were carefully monitored throughout the whole experiment to minimize pain.

2.3. CCI-induced rat model of neuropathic pain

All SD rats were anesthetized under 4–5% sevoflurane (Hengrui Pharmaceuticals Co., Ltd., Jiangsu, China) (The oxygen flow was set at 2 L/min and the FiO2 at 0.4). Following the method described by Bennett and Xie [24], the rats were positioned prone, and the fur in the right surgical area was removed. After disinfection and draping, the skin was incised, and the intermuscular space between the biceps femoris was carefully separated to expose the right sciatic nerve. The sciatic nerve was gently dissected from surrounding tissues. Using 4-0 chromic gut suture soaked in physiological saline for at least 30 min, loose ligations were performed by wrapping the suture around the midsection of the main trunk of the sciatic nerve. During each ligation, blood supply was not completely interrupted, and there was slight tremor in the right lower limb. Ligation was performed every 1 mm for a total of 4 times. The muscles and skin were then sutured and penicillin G sodium was administered prophylactically to prevent infection. All procedures were carried out by the same person following aseptic principles to ensure consistency in both the surgical incision and the degree of nerve ligation for modelling purposes. Rats in the Sham + Saline group (S & S) were given the same surgery except that nerves were ligated.

2.4. Experimental design and grouping

Based on preliminary results and previous literature, the success rate of CCI modelling was estimated to be 70 %. Considering the bilateral significance level of $\alpha = 0.05$ and power = 90 % ($\beta = 0.10$), sample size calculation using PASS 15.0 determined that each group would require 10 rats, taking into account a 10 % loss due to errors, modelling success rate, and other experimental requirements. Therefore, a total of 43 rats were included in the study, and 3 SD rats with abnormal basal PMWT value were eliminated before grouping. After grouping, 2 SD rats with self-mutilation (during Day 7–15 after surgery) and 8 SD rats with unsuccessful modelling (on Day 7 after surgery) were further eliminated. Finally, the remaining 30 SD rats were randomly allocated into 3 groups according to a random number table, including the S & S group (n = 10), the C & S group (n = 10) and the C&U group (n = 10) (Fig. 1A).

Day 0 (T_0) was recorded as the day of modelling. Behavioral tests were conducted on day 0 (before modelling) and days 1, 3, 5, 7, 9, 11, 13 and 15 (denoted as $T_{1,3,5,7,9,11,13,15}$) after modelling (Fig. 1B). Rats with the baseline paw mechanical pain threshold (T_0 PMWT) below 2 standard deviations of the mean baseline PMWT were considered to have abnormal pain perception and were excluded from subsequent grouping and modelling, meanwhile, if the PMWT on the 7th day was less than 2 standard deviations below the basal value, the rats were considered neuropathic, and those rats that did not meet the above criteria were considered failed preparations [25]. The SD rats were randomly divided into three groups: (1) Sham + Saline group (the S&S group); (2) CCI + Saline group (the C&S group);

and (3) CCI + HUC-MSCs group (the C&U group). In the S&S group, only to the right sciatic nerve trunk was located without a ligation being made, while CCI rats (the C&S group and the C&U group) were administered a right sciatic nerve trunk ligation. On T_7 after modelling, 200 μl sterile saline was injected via caudal vein in the S&S and the C&S group after the behavioural tests, while HUC-MSCs (1×10^6 cells in 200 μl sterile saline) was transplanted in the C&U groups.

2.5. Behavioral evaluations

Before each pain behavioral test, the rats were observed for walking gait, standing posture, local skin condition, mobility, muscle tone, and the presence of self-injury. If signs of lower limb paralysis, dragging of the hind limbs, or self-mutilation behavior such as toe biting were observed during the observation period, it was considered indicative of excessive nerve ligation injury, and those rats were excluded from the experiment.

The rats were placed in a special plexiglass cage with a mesh bottom for 30 min until they were quiet. The up-down method was used to measure the 50 % PWMT with a Von Frey filament (0.04–15.0 g, IITC Life Science Inc., California, USA), as described by Chaplan et al. [25]. Starting from a force of 2.0 g, stimulate the glabrous area of the right palmoplantar surface of rats, and the Von Frey hair was in the shape of "S" for a duration of 6–8 s with an interval of 5 min between adjacent stimulations. During the stimulation time, the rat raised or licked the right foot as a positive response, which was represented by "X", whereas no response is recorded by "O." If there was no response to the first fiber stimulation, a fiber with a higher force level was applied; if there was a response, a fiber with a lower force level was used. This process was repeated until five measurements were taken starting from the first response, resulting in a sequence of combinations of "O" and "X", and the k value of this sequence obtained from the table and the strength (f) of the last fiber was entered into the formula to calculate the PMWT of the rat.

Preheat the temperature-controlled glass plate for 30 min to maintain it at around 30 °C, and the rats were acclimated to the environment for more than 30 min. The testing was started when the rats were in an awake and calm state. TWL was measured via the Hargreaves Test (Model 390G, IITC Life Science Inc.) as reported by Hargreaves et al. [26], the 40 % maximum light intensity thermal radiation beam was positioned on the middle posterior third of the right plantar surface of the rat. Record the time when the rat showed withdrawal, licking, foot lifting, or paw shaking as the paw withdrawal latency, with a cut-off time of 20 s to prevent injury. Repeat the measurement five times, with a 5-min interval between each measurement, and the average value of the remaining three measurements was taken as the TWL of the rat after excluding the maximum and minimum values. All measurements were performed by the same blinded person.

2.6. Western-blotting analysis

On day 15 after behavioral evaluations, SD rats were infused with 150 ml ice saline via the left ventricle after anesthetized with 4 % sevoflurane, and samples of the right L4-5 spinal cord were quickly isolated and collected on the ice box. After protein extraction, the sample lysates were separated by SDS-PAGE and transferred onto PVDF membranes (Millipore, Massachusetts, USA). The membranes were placed in a shaker with a rotating speed of 50–60 rpm/min and blocked by 5 % skim milk for 2 h at room temperature (RT), then incubated with primary antibodies of a rabbit polyclonal antibody anti-ionized calcium-binding adapter molecule 1 (Iba-1, ab5076, 1:2000; Abcam, Cambridge, UK) and Anti-Beta-Actin Monoclonal Loading Control Antibody (β-actin, G043, 1:2000; ABM good, British Columbia, Canada) overnight at 4 °C. Next, the membranes were incubated with HRP-conjugated Goat Anti-Mouse or Rabbit anti-Goat IgG (1:5000; ZSGB-BIO, Beijing, China) for 1 h at RT with a rotating speed of 50–60 rpm/min in a shaker. A Chemiluminescence imaging system (BIO-RAD, California, USA) was used to detect the labelled protein and signal intensity was measured with Image J software (National Institutes of Health, Maryland, USA). Western-blotting analyses were replicated in three independent experiments.

2.7. Immunofluorescent (IF) staining

On day 15 after behavioral evaluations, rats were infused with 150 ml ice saline and subsequently with 100 ml 4 % paraformaldehyde (PFA; Sigma-Aldrich, Missouri, USA) via the left ventricle after being anesthetized with 4 % sevoflurane. Next, the L4-5 spinal cord was cut into approximately 5 mm × 5 mm × 3 mm bite-sizes and fixed overnight in 4 % PFA (Sigma-Aldrich, Missouri, USA) at 4 °C. After dehydration, wax leaching and embedding, the samples were cut into 4 μm paraffin slices. After that, the paraffin slices were dewaxed, antigen repaired, serum sealed, and subsequently treated with anti-Iba-1 (ab153696, 1:200; Abcam) at 4 °C overnight. The paraffin slices were then incubated with the FITC-conjugated donkey anti-rabbit IgG (1:300; Servicebio, Hubei, China) for 50 min at RT in the dark, followed by DAPI (Servicebio) incubation for nuclei labelling for 10 min. Finally, the slices were observed and photographed under a fluorescence microscope (Nikon, Japan), and Image J software (National Institutes of Health, USA) was used to analyze the fluorescent imaging of Iba-1.

2.8. Transmission electron microscope (TEM) analysis

On day 15 after behavioral evaluations, rats were sacrificed under 8 % sevoflurane. The sciatic nerves at the ligation site were collected quickly and placed in a wax block filled with 2.5 % glutaraldehyde and trimmed to 1 mm^3. The resin blocks were then cut into 90–100 nm sections on the ultra-microtome (Leica, Germany) after post-fixation, dehydration, resin penetration and embedding, and polymerization. Then the sections were stained, examined, and photographed by transmission electron microscopy (FEI Company, Oregon, USA) in the Fujian Medical University Electron Microscopy Unit.

2.9. Statistical analysis

Statistical analyses were performed with IBM SPSS 16.0. All metrological data were subjected to normality testing, and conforming to normal distribution was presented as mean ± standard deviation (mean ± SD). Comparison of the PMWT and TWL was conducted using generalized estimating equations, and the results of WB and the immunofluorescence were analyzed by one-way analysis of variance, followed by Tukey's HSD test. Variables with $P < 0.05$ were considered as statistically significant. GraphPad Prism 8.0 (GraphPad Software, Massachusetts, USA) was used for mapping.

3. Results

3.1. General behavioral observations

Before surgery, all rats in each group displayed normal walking and standing posture. However, 3 rats with abnormal pain perception were excluded from the subsequent experiments. On T_7, 8 rats did not meet the diagnostic criteria for neuropathic pain, while 2 rats exhibited self-injury during the observation period, and these rats were excluded from the following study. The remaining rats in both the C&S group and the C&U group showed behavioral abnormalities on the ligation side of rats, such as toes folded together, foot valgus, and standing on the contralateral side (Fig. 2A & Fig. 2B-left side). In comparison, the SD rats in the S&S group revealed no obvious behavioral abnormalities after modelling (Fig. 2B-right side).

Intravenous infusion of HUC-MSCs significantly ameliorated CCI-induced mechanical allodynia and thermal hyperalgesia.

Using generalized estimating equation analysis, statistically significant differences were found between PMWT and TWL values among the three groups of rats at different time points ($P < 0.001$). Additionally, there was an interaction effect between groups and time points ($P < 0.001$). In terms of separate effects, there was no statistically significant difference in PMWT and TWL at different time points within the S&S group. In the C&S group, the value of ipsilateral PWMT decreased from the first day after modelling (14.20 ± 1.28 g [T_0] to 9.72 ± 4.99 g [T_1]), reached neuropathic pain criteria on day 3 (3.98 ± 3.27 g, T_3), and was then persistently maintained at a low level until the end of experiment (1.36 ± 0.98 g, day 15, T_{15}), which was significantly lower than values in the S&S group ($P < 0.01$) (Fig. 3A). Similarly, the value of TWL in the C&S group decreased from 16.52 ± 5.04 s (T_0) to 13.35 ± 3.72 s on day 5 (T_5), and was persistently maintained until day 15 (11.18 ± 6.13 s, T_{15}) when compared with the S&S group ($P < 0.01$) (Fig. 3B). To investigate the effects of HUC-MSCs on CCI-induced neuropathic pain, SD rats in the C&U group were injected intravenously with HUC-MSCs on day 7 when allodynia and hyperalgesia were most prominent, at which time both PWMT and TWL were significantly decreased compared with the S&S group ($P < 0.01$). Significantly, we found a gradual amelioration of mechanical hyperalgesia in the C&U group from 1.93 ± 1.35 g (T_7) to 8.37 ± 5.60 g (T_{15}). Compared with the C&S group, ipsilateral PWMT in the C&U group was significantly increased on days 13 (T_{13}) and 15 (T_{15}) ($P < 0.01$). However, when compared to the S&S group, ipsilateral PWMT in the C&U group did not return to a baseline level, and the difference was still statistically significant ($P < 0.01$) (Fig. 3A). Meanwhile, the thermal allodynia in the C&U group gradually decreased from 12.70 ± 4.78 s (T_7) to 16.69 ± 4.24 s (T_{15}), which was significantly higher than those in the C&S group ($P < 0.01$). Additionally, there was no statistically significant difference in TWL value between the C&U group and the S&S group ($P > 0.05$) (Fig. 3B).

3.2. CCI-induced activation of microglia was efficiently suppressed by intravenous infusion of HUC-MSCs

To further verify the potential influence of systemic administration of HUC-MSCs upon microglia activation, we took advantage of western-blotting and immunofluorescent staining analyses. By conducting immunofluorescent staining, we found that the abnormally

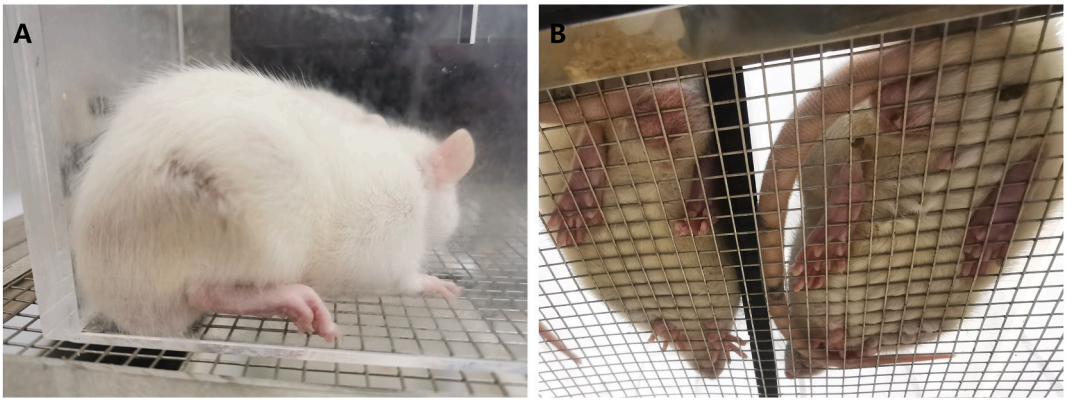

Fig. 2. General behavioural observations in different groups of rats. **A:** After the successful modelling of CCI, the ligation side (right side) of rats showed some abnormal behavioural changes, such as toes curling together, foot valgus, and standing on the contralateral side. **B:** Right side: S&S group, normal standing posture. Left side: CCI modelling showed behavioural abnormalities.

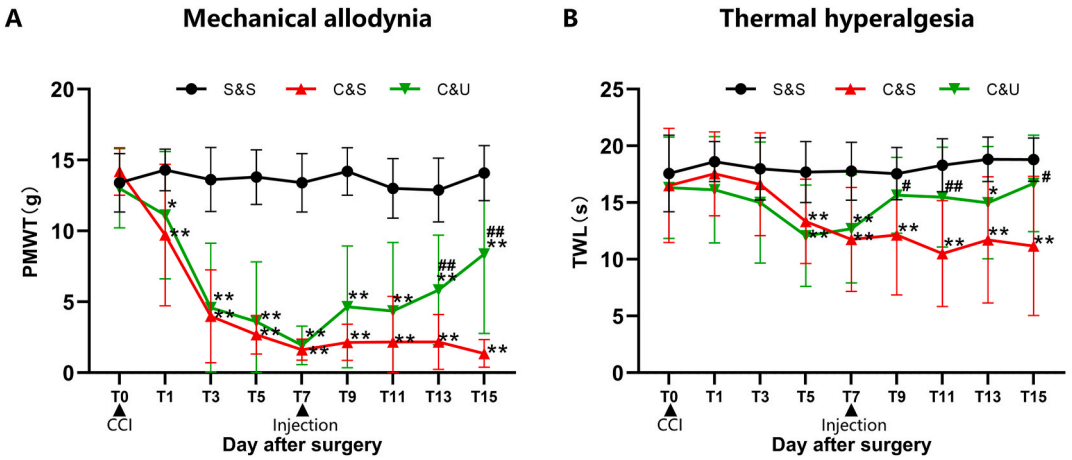

Fig. 3. HUC-MSCs ameliorated CCI-induced mechanical allodynia and thermal hyperalgesia in ipsilateral limb Paw withdrawal mechanical threshold (PMWT, A) and thermal withdrawal latency (TWL, B) were significantly reduced in rats with successful modelling by sciatic nerve ligation, and CCI-induced mechanical allodynia and thermal hyperalgesia were reversible by intravenous injection of HUC-MSCs on day 7 after modelling. The PMWT and TWL gradually increased from day 7 (T7) until the end of the experiment (day 15, T15) in the C&U group. Compared with S&S group, $^{*}P < 0.05$, $^{**}P < 0.01$; compared with C&S group, $^{\#}P < 0.05$, $^{\#\#}P < 0.01$. The data are expressed as mean ± SD ($n = 10$ per group).

elevated expression of Iba-1 (a marker of activated microglia) in the dorsal horn of the spinal cord after CCI was sharply decreased after HUC-MSCs treatment in the C&U group (Fig. 4A&B). Specifically, the expression of Iba-1 protein was upregulated from 0.57 ± 0.13 in the S&S group to 1.02 ± 0.11 ($P < 0.05$) in the C&S group on day 15, whereas the value decreased from 1.02 ± 0.11 to 0.63 ± 0.14 in the C&U group with HUC-MSCs administration ($P < 0.05$) (Fig. 4C). Collectively, the activation of microglia after CCI was significantly suppressed by intravenous injection of HUC-MSCs.

3.3. *Ultrastructure observations of sciatic nerve*

To observe the ameliorative effect of HUC-MSCs upon the sciatic nerve, transmission electron microscope (TEM) analysis was employed. As shown in Fig. 5, the sciatic nerve revealed a typical ultrastructure in the S&S group, including a thick and compact myelin sheath, unmyelinated fibres, and enclosing myelinated fibres in Schwann cells (Fig. 5A&B). Differing from the S&S group, obvious degenerative changes were found in the ligation site of sciatic nerves in the C&S group such as demyelination of sciatic nerve fibres, twisted myelin sheaths with damaged laminate structure, atrophied axon and myelin whorls engulfed by infiltrating macrophages (Fig. 5C&D). Strikingly, the structure of the myelin sheath was basically intact in the C&U group, including the typical segmental and occasional plaque demyelination, together with vacuolation of axoplasm and new small thin myelinated fibres (Fig. 5E&F).

4. Discussion

In recent years, a growing amount of evidence has suggested the efficacy of HUC-MSCs for the significant remission of mechanical allodynia and thermal hyperalgesia in different models of neuropathic pain due to their superiority in long-term proliferation, low immunogenicity [11], anti-inflammatory effect [12], and high tissue survival ability [13]. In terms of drug delivery strategy, previous research suggested that most MSCs delivered through intravenous injection would be deposited in the lungs and fail to reach the targeted sites of neuropathic pain, while immune cells in circulation would also directly damage these cells, resulting in a significant reduction in therapeutic efficacy [18,19]. Currently, there are limited reports on intravenous infusion of HUC-MSCs for peripheral neuropathic pain treatment. For example, Miyano et al. [20] found that rats with partial sciatic nerve ligation showed relief from pain hypersensitivity on the second day following a single intravenous injection of HUC-MSCs. Instead, Liu and the colleagues verified the significant improvement in PMWT only after 14 days of MSC injection [21]. Thus, it's interesting to further verify the therapeutic efficacy of intravenous administration, which would also benefit clinical implementation due to the advantages including less invasive and more convenient. Therefore, in comparison to the existing literatures reporting intrathecal administration [14–16,27], we focused on the therapeutic effects and possible mechanism of intravenous HUC-MSC administration, and our findings preliminarily verified the feasibility of systemic infusion of HUC-MSCs for ameliorating CCI-induced neuropathic pain in SD rats via suppressing the microglia-mediated regulatory mechanism.

In this study, a series of modifications and optimizations were conducted. For instance, as to the time point selected for the administration of HUC-MSCs, we chose the day on which allodynia appeared most obviously after CCI in rats (on Day 7) based on pre-experiments and previous studies [28]. To avoid cell damage and decreased viability of HUC-MSCs, we optimized the cell suspension procedure and the transplanted cell number (1×10^6 cells in 200 μl saline) to avoid forming clusters in the microinjection cannula [29,30]. Interestingly, a single systemic infusion of HUC-MSCs (1×10^6) revealed comparable anti-nociceptive effects as intrathecal

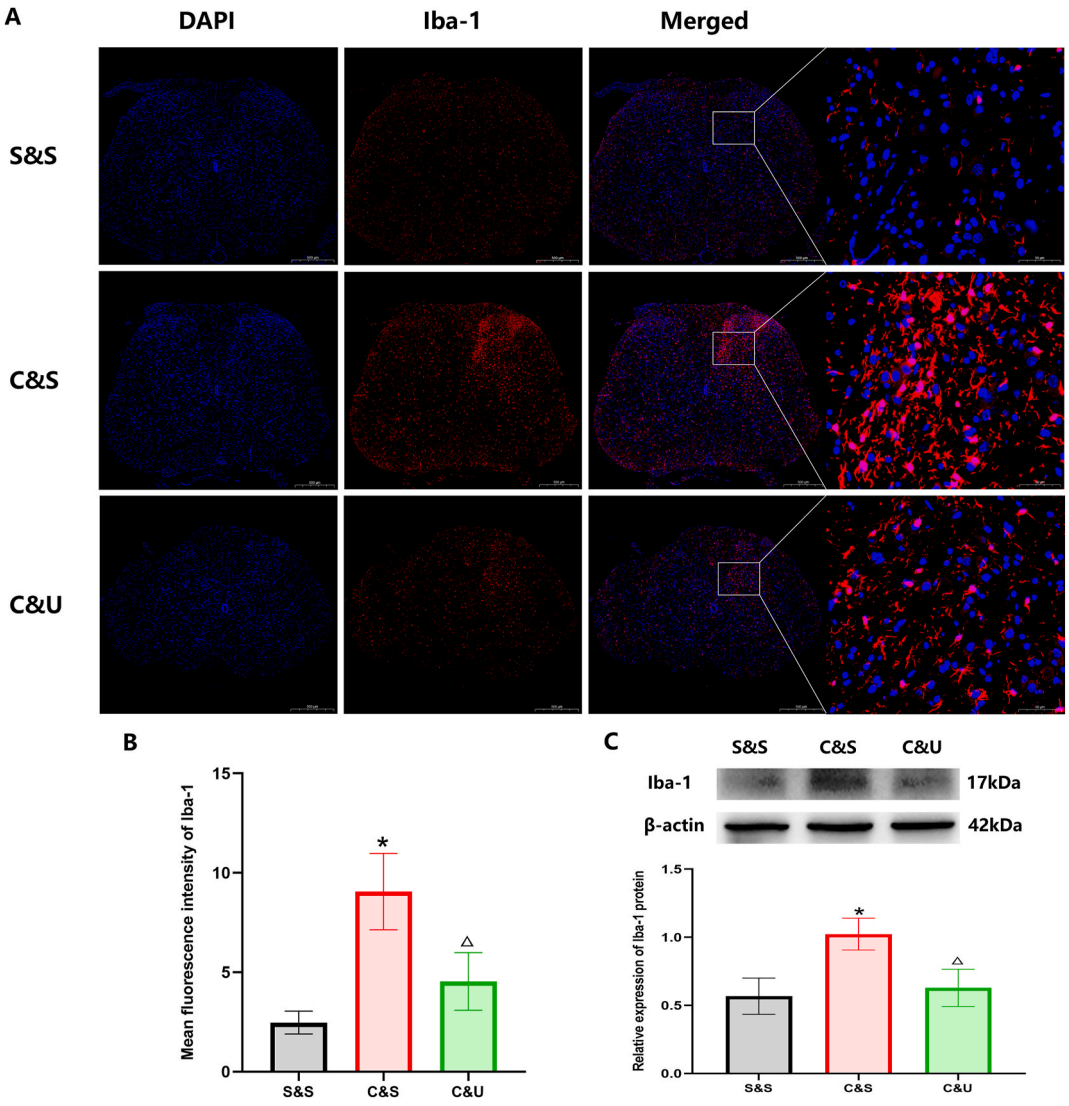

Fig. 4. Effect of HUC-MSCs on the expression of ionized calcium-binding adapter molecule 1 (Iba-1) in the spinal cord horn on day 15 after CCI Representative immune-histological staining of the nucleus marker DAPI and the microglial marker Iba-1 on the ipsilateral side of the L4-5 spinal cord (scale bar 500 μm) on day 15 after CCI with or without intravenous injection of HUC-MSCs. Mean fluorescence intensity of Iba-1 in the dorsal horn is shown in B. Representative Western blot analysis of Iba-1 and the level of relative expression of Iba-1 by densitometric analysis is shown in C. Compared with S&S group, $^{*}P < 0.05$; compared with C&S group, $^{\triangle}P < 0.05$. Values are expressed as mean ± SD ($n = 3$ per group).

injection and could last for at least 7 days [14], which was consistent with the results of Miyano et al., who intravenously transplanted 5 times HUC-MSCs (5×10^6) into PSNL rats [20]. Notably, we found a significant increase in TWL in the C&U group on two post-administration days, with a faster recovery than PMWT, which was consistent with the report by Liu et al. [21] It is believed that thermal hyperalgesia is primarily caused by peripheral mechanisms, while HUC-MSCs administered intravenously can direct themselves to the damaged sciatic nerve and exert anti-inflammatory effects as peripheral circulating stem cells. Furthermore, with the aid of TEM analysis, we verified the resumption of myelin lamellar structure of the sciatic nerve and the formation of new myelin sheath, together with the significant improvement in myelin basic protein levels after HUC-MSC administration [20] and the potential ability of tonsilla-derived MSCs to directly differentiate into Schwann cells and promote peripheral nerve regeneration [31], which collectively indicated the complexity of the underlying molecular mechanism in mediating the therapeutic effect of HUC-MSCs during nerve regeneration and nerve injury repairment.

Recent research has suggested the involvement of immune cells in the formation and maintenance of neuropathic pain, and in particular, inhibiting the activation of microglia, reducing the polarization of microglia towards pro-inflammatory phenotypes, and decreasing the level of spinal inflammatory factors such as IL-1β and TNF-α, making this a promising area of study for the treatment of neuropathic pain [32–35]. In this study, we found that CCI induced an increase in Iba-1-positive cells in the ipsilateral spinal cord dorsal horn, which suggested that the infiltration of microglia cells into the spinal dorsal horn is attributable to CCI-induced neuronal

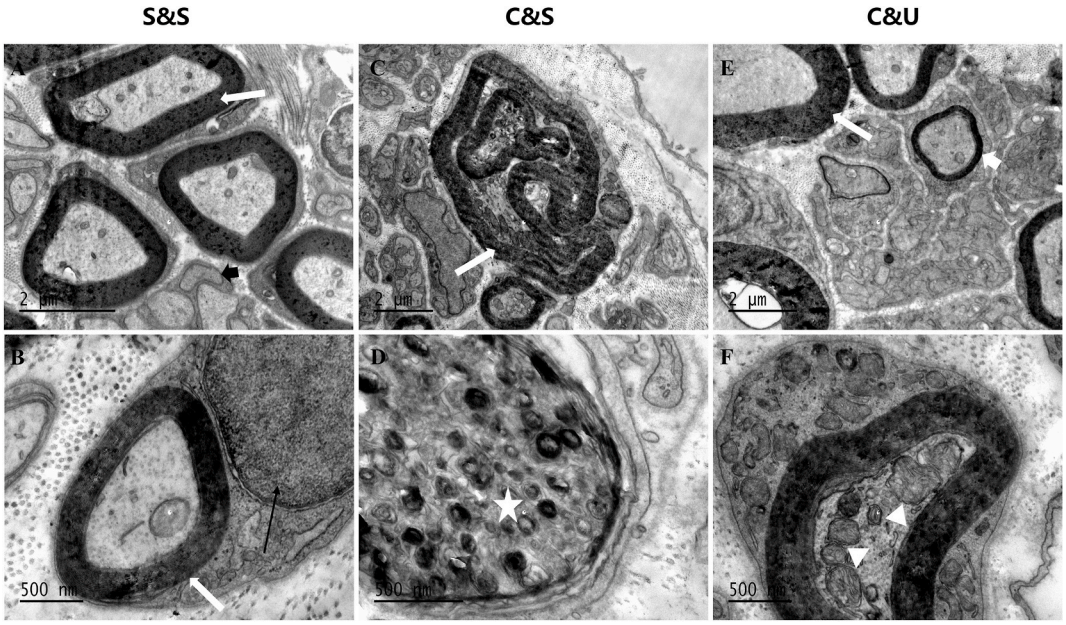

Fig. 5. Electron micrographs of right ligation of sciatic nerve. Dense and intact myelinated fibres (white arrow), unmyelinated nerve fibres (thick black arrow), and myelinated fibres enclosed by Schwann cells (thin black arrow) were found in the S&S group (A and B). Twisted and degenerated myelin sheath (white arrow) and infiltrating macrophage (white star) engulfing degenerated myelin whorls were observed in the C&S group (C and D). Occasional loose fuzzy fragments in the lamellar structure (white arrow) and vacuole formation in the axoplasm (white triangle), accompanied by the formation of new myelin sheath (thick white arrow), was observed in the C&U group.

damage. Strikingly, HUC-MSCs infusion intravenously could significantly reverse the accumulation of activated microglia, which was consistent with the results of Chen et al. by intrathecal injection [14]. Interestingly, Miyano et al. also indicated a decline in macrophages activation in the DRG of PSNL rats after HUC-MSCs administration [20]. Taken together, these data suggested the inhibitory effect of HUC-MSCs upon immune cell activity in neuropathic pain at both a peripheral and central level. Therefore, it is crucial to further analyze the systemic changes in the immune inflammatory microenvironment from the periphery to the central nervous system after HUC-MSCs treatment, and this will also be the focus of our subsequent research.

Nevertheless, there are still several unresolved issues in this study, which are also crucial points that need to be further clarified before large-scale clinical application. For instance, the specific details of the application dosage and administration frequency, together with the long-term therapeutic effects of HUC-MSCs upon peripheral neuropathic pain, need to be explored in details in the future. Meanwhile, the elucidation of the underlying mechanism on HUC-MSCs-based cytotherapy for peripheral neuropathic pain is also urgently needed before clinical transformation. Therefore, in subsequent studies, we will prolong the observation period to assess the sustained efficacy of single-dose administration and determine if multiple injections yield better results, as well as utilize multifaceted techniques such as proteomics and flow cytometry to delve into a series of protein expression, phenotypic polarization, and downstream inflammatory factor expression after inhibiting spinal microglial cell activation through intravenous administration of HUC-MSCs. In addition, we have previously established a high-efficient procedure for large-scale generation of $CD106^{+}$ HUC-MSCs, a novel cell subtype with increased proangiogenic potential, preferable immunomodulatory properties and enhanced homing capability [22]. Thus, in future work, we will use the cell subtype and its exosomes to conduct in-depth research on the mechanism of neuropathic pain treatment using data obtained from this study.

5. Conclusions

Overall, we verified that mechanical allodynia and thermal hyperalgesia induced by chronic constriction injury of the sciatic nerve during neuropathic pain can be significantly reduced by a single intravenous injection of HUC-MSCs. Being that intravenous injection is the most common used mode of administration in the clinic, this indicates the feasibility of the systemic infusion of HUC-MSC for ameliorating the CCI-induced neuropathic pain. In addition, the antinociceptive effects of HUC-MSCs were found to be partially mediated by suppressing the abnormal activation of microglia in the ipsilateral spinal dorsal horn and the repairment of sciatic nerve injury. Our findings will help further explore the biofunction and the concomitant mechanism of HUC-MSCs for neuropathic pain administration, and thus provide new references and perspectives for clinical application and promotion in the future.

Ethical statement

All experiments in this study were carried out in accordance with the US National Institutes of Health Guide for the Care and Use of

Laboratory Animals and were approved by the Administration Committee of Experimental Animals of Fujian Medical University (No. FJMU IACUC 2021-0490).

Data availability statement

The datasets for this study can be found in the FigShare [DOI: 10.6084/m9.figshare.25331581]

CRediT authorship contribution statement

Xiaodong Xu: Writing – original draft, Methodology, Investigation. **Hui Chen:** Methodology, Investigation, Data curation. **Yubei Qiu:** Software, Funding acquisition, Data curation. **Ye Chen:** Software, Methodology, Formal analysis, Data curation. **Junle Liu:** Supervision, Data curation. **Bangwei Zeng:** Software, Formal analysis, Data curation. **Lei Lin:** Methodology, Data curation. **Xinyan Lin:** Formal analysis. **Leisheng Zhang:** . **Liangcheng Zhang:** Writing – review & editing, Project administration, Funding acquisition, Conceptualization.

Declaration of competing interest

The authors declare that they have no known competing financial interests or personal relationships that could have appeared to influence the work reported in this paper.

Acknowledgement

This work was supported by grants from General Project of Natural Science Foundation of Fujian Province (2021J01776, 2021J01806), and the Key Clinical Specialty Discipline Construction Program of Fujian Medical University Union Hospital (0252004), Natural Science Foundation of Jiangxi Province (20224BAB206077, 20212BAB216073), and Postdoctoral Program of Natural Science Foundation of Gansu Province (23JRRA1319). The coauthors would also thank the members in Fujian Medical University Union Hospital for their technical support.

Appendix A. Supplementary data

Supplementary data to this article can be found online at https://doi.org/10.1016/j.heliyon.2024.e32689.

References

[1] R.D. Treede, T.S. Jensen, J.N. Campbell, G. Cruccu, J.O. Dostrovsky, J.W. Griffin, P. Hansson, R. Hughes, T. Nurmikko, J. Serra, Neuropathic pain: redefinition and a grading system for clinical and research purposes, Neurology 70 (2008) 1630–1635, https://doi.org/10.1212/01.wnl.0000282763.29778.59.
[2] T.S. Jensen, R. Baron, M. Haanpaa, E. Kalso, J.D. Loeser, A. Rice, R.D. Treede, A new definition of neuropathic pain, Pain 152 (2011) 2204–2205, https://doi.org/10.1016/j.pain.2011.06.017.
[3] E. Cavalli, S. Mammana, F. Nicoletti, P. Bramanti, E. Mazzon, The neuropathic pain: an overview of the current treatment and future therapeutic approaches, Int. J. Immunopathol. Pharmacol. 33 (2019) 1681075631, https://doi.org/10.1177/2058738419838383.
[4] M.W. Salter, S. Beggs, Sublime microglia: expanding roles for the guardians of the cns, Cell 158 (2014) 15–24, https://doi.org/10.1016/j.cell.2014.06.008.
[5] R.E. Zigmond, F.D. Echevarria, Macrophage biology in the peripheral nervous system after injury, Prog. Neurobiol. 173 (2019) 102–121, https://doi.org/10.1016/j.pneurobio.2018.12.001.
[6] O. Chen, C.R. Donnelly, R. Ji, Regulation of pain by neuro-immune interactions between macrophages and nociceptor sensory neurons, Curr. Opin. Neurobiol. 62 (2020) 17–25, https://doi.org/10.1016/j.conb.2019.11.006.
[7] Y. Sun, T. Wang, Q. Hu, W. Zhang, Y. Zeng, X. Lai, L. Zhang, M. Shi, Systematic comparation of the biological and transcriptomic landscapes of human amniotic mesenchymal stem cells under serum-containing and serum-free conditions, Stem Cell Res. Ther. 13 (2022) 490, https://doi.org/10.1186/s13287-022-03179-2.
[8] L. Zhang, Y. Wei, Y. Chi, D. Liu, S. Yang, Z. Han, Z. Li, Two-step generation of mesenchymal stem/stromal cells from human pluripotent stem cells with reinforced efficacy upon osteoarthritis rabbits by ha hydrogel, Cell Biosci. 11 (2021) 6, https://doi.org/10.1186/s13578-020-00516-x.
[9] S. Asgharzade, A. Talaei, T. Farkhondeh, F. Forouzanfar, A review on stem cell therapy for neuropathic pain, Curr. Stem Cell Res. Ther. 15 (2020) 349–361, https://doi.org/10.2174/1574888X15666200214112908.
[10] E.A. Kimbrel, N.A. Kouris, G.J. Yavanian, J. Chu, Y. Qin, A. Chan, R.P. Singh, D. Mccurdy, L. Gordon, R.D. Levinson, R. Lanza, Mesenchymal stem cell population derived from human pluripotent stem cells displays potent immunomodulatory and therapeutic properties, Stem Cell. Dev. 23 (2014) 1611–1624, https://doi.org/10.1089/scd.2013.0554.
[11] D. Kim, M. Staples, K. Shinozuka, P. Pantcheva, S. Kang, C.V. Borlongan, Wharton's jelly-derived mesenchymal stem cells: phenotypic characterization and optimizing their therapeutic potential for clinical applications, Int. J. Mol. Sci. 14 (2013) 11692–11712, https://doi.org/10.3390/ijms140611692.
[12] Y.J. Jeon, J. Kim, J.H. Cho, H.M. Chung, J.I. Chae, Comparative analysis of human mesenchymal stem cells derived from bone marrow, placenta, and adipose tissue as sources of cell therapy, J. Cell. Biochem. 117 (2016) 1112–1125, https://doi.org/10.1002/jcb.25395.
[13] M. Yousefifard, F. Nasirinezhad, M.H. Shardi, A. Janzadeh, M. Hosseini, M. Keshavarz, Human bone marrow-derived and umbilical cord-derived mesenchymal stem cells for alleviating neuropathic pain in a spinal cord injury model, Stem Cell Res. Ther. 7 (2016) 36, https://doi.org/10.1186/s13287-016-0295-2.
[14] C. Chen, F. Chen, C. Yao, S. Shu, J. Feng, X. Hu, Q. Hai, S. Yao, X. Chen, Intrathecal injection of human umbilical cord-derived mesenchymal stem cells ameliorates neuropathic pain in rats, Neurochem. Res. 41 (2016) 3250–3260. https://doi:10.1007/s11064-016-2051-5.
[15] S. Shiue, R. Rau, H. Shiue, Y. Hung, Z. Li, K.D. Yang, J. Cheng, Mesenchymal stem cell exosomes as a cell-free therapy for nerve injury-induced pain in rats, Pain 160 (2019) 210–223, https://doi.org/10.1097/j.pain.0000000000001395.
[16] X. Gao, L. Gao, X. Kong, Y. Zhang, S. Jia, C. Meng, Mesenchymal stem cell-derived extracellular vesicles carrying mir-99b-3p restrain microglial activation and neuropathic pain by stimulating autophagy, Int. Immunopharm. 115 (2023) 109695, https://doi.org/10.1016/j.intimp.2023.109695.

[17] L. Priano, G.P. Zara, N. El-Assawy, S. Cattaldo, E. Muntoni, E. Milano, L. Serpe, C. Musicanti, C. Pérot, M.R. Gasco, G. Miscio, A. Mauro, Baclofen-loaded solid lipid nanoparticles: preparation, electrophysiological assessment of efficacy, pharmacokinetic and tissue distribution in rats after intraperitoneal administration, Eur. J. Pharm. Biopharm. 79 (2011) 135–141, https://doi.org/10.1016/j.ejpb.2011.02.009. Official Journal of Arbeitsgemeinschaft Fur Pharmazeutische Verfahrenstechnik E.V.
[18] L. Liu, Z. Hua, J. Shen, Y. Yin, J. Yang, K. Cheng, A. Liu, L. Wang, J. Cheng, Comparative efficacy of multiple variables of mesenchymal stem cell transplantation for the treatment of neuropathic pain in rats, Mil. Med. 182 (2017) 175–184, https://doi.org/10.7205/MILMED-D-16-00096.
[19] G. Sezer, A.H. Yay, Z.S. Sarica, Z.B. Gonen, G.O. Onder, A. Alan, S. Yilmaz, B. Saraymen, D. Bahar, Bone marrow-derived mesenchymal stem cells alleviate paclitaxel-induced mechanical allodynia in rats, J. Biochem. Mol. Toxicol. 36 (2022) e23207, https://doi.org/10.1002/jbt.23207.
[20] K. Miyano, M. Ikehata, K. Ohshima, Y. Yoshida, Y. Nose, S. Yoshihara, K. Oki, S. Shiraishi, M. Uzu, M. Nonaka, Y. Higami, Y. Uezono, Intravenous administration of human mesenchymal stem cells derived from adipose tissue and umbilical cord improves neuropathic pain via suppression of neuronal damage and anti-inflammatory actions in rats, PLoS One 17 (2022) e0262892, https://doi.org/10.1371/journal.pone.0262892.
[21] M. Liu, W. Yu, F. Zhang, T. Liu, K. Li, M. Lin, Y. Wang, G. Zhao, J. Jiang, Fe(3)o(4)@polydopamine-labeled mscs targeting the spinal cord to treat neuropathic pain under the guidance of a magnetic field, Int. J. Nanomed. 16 (2021) 3275–3292, https://doi.org/10.2147/IJN.S296398.
[22] Y. Wei, L. Zhang, Y. Chi, X. Ren, Y. Gao, B. Song, C. Li, Z. Han, L. Zhang, Z. Han, High-efficient generation of vcam-1(+) mesenchymal stem cells with multidimensional superiorities in signatures and efficacy on aplastic anaemia mice, Cell Prolif. 53 (2020) e12862, https://doi.org/10.1111/cpr.12862.
[23] Q. Zhao, L. Zhang, Y. Wei, H. Yu, L. Zou, J. Huo, H. Yang, B. Song, T. Wei, D. Wu, W. Zhang, L. Zhang, D. Liu, Z. Li, Y. Chi, Z. Han, Z. Han, Systematic comparison of huc-mscs at various passages reveals the variations of signatures and therapeutic effect on acute graft-versus-host disease, Stem Cell Res. Ther. 10 (2019) 354, https://doi.org/10.1186/s13287-019-1478-4.
[24] G.J. Bennett, Y. Xie, A peripheral mononeuropathy in rat that produces disorders of pain sensation like those seen in man, Pain 33 (1988) 87–107, https://doi.org/10.1016/0304-3959(88)90209-6.
[25] S.R. Chaplan, F.W. Bach, J.W. Pogrel, J.M. Chung, T.L. Yaksh, Quantitative assessment of tactile allodynia in the rat paw, J. Neurosci. Methods 53 (1994) 55–63. http://doi:10.1016/0165-0270(94)90144-9.
[26] K. Hargreaves, R. Dubner, F. Brown, C. Flores, J. Joris, A new and sensitive method for measuring thermal nociception in cutaneous hyperalgesia, Pain 32 (1988) 77–88, https://doi.org/10.1016/0304-3959(88)90026-7.
[27] X. Gao, L. Gao, Y. Zhang, X. Kong, S. Jia, C. Meng, Huc-mscs-derived exosomes attenuate neuropathic pain by inhibiting activation of the tlr2/myd88/nf-κb signaling pathway in the spinal microglia by targeting rsad2, Int. Immunopharm. 114 (2023) 109505, https://doi.org/10.1016/j.intimp.2022.109505.
[28] Y. Sun, D. Zhang, H. Li, R. Long, Q. Sun, Intrathecal administration of human bone marrow mesenchymal stem cells genetically modified with human proenkephalin gene decrease nociceptive pain in neuropathic rats, Mol. Pain 13 (2017) 2071462075, https://doi.org/10.1177/1744806917701445.
[29] H. Kim, H.Y. Kim, M.R. Choi, S. Hwang, K. Nam, H. Kim, J.S. Han, K.S. Kim, H.S. Yoon, S.H. Kim, Dose-dependent efficacy of als-human mesenchymal stem cells transplantation into cisterna magna in sod1-g93a als mice, Neurosci. Lett. 468 (2010) 190–194, https://doi.org/10.1016/j.neulet.2009.10.074.
[30] F. Forouzanfar, B. Amin, A. Ghorbani, H. Ghazavi, F. Ghasemi, K. Sadri, S. Mehri, H.R. Sadeghnia, H. Hosseinzadeh, New approach for the treatment of neuropathic pain: fibroblast growth factor 1 gene-transfected adipose-derived mesenchymal stem cells, Eur. J. Pain 22 (2018) 295–310, https://doi.org/10.1002/ejp.1119.
[31] N. Jung, S. Park, Y. Choi, J. Park, Y.B. Hong, H.H.C. Park, Y. Yu, G. Kwak, H.S. Kim, K. Ryu, J.K. Kim, I. Jo, B. Choi, S. Jung, Tonsil-derived mesenchymal stem cells differentiate into a schwann cell phenotype and promote peripheral nerve regeneration, Int. J. Mol. Sci. 17 (2016). http://doi:10.3390/ijms17111867.
[32] G. Chen, Y. Zhang, Y.J. Qadri, C.N. Serhan, R. Ji, Microglia in pain: detrimental and protective roles in pathogenesis and resolution of pain, Neuron 100 (2018) 1292–1311, https://doi.org/10.1016/j.neuron.2018.11.009.
[33] J. Yuan, Y. Fei, Lidocaine ameliorates chronic constriction injury-induced neuropathic pain through regulating m1/m2 microglia polarization, Open Med. 17 (2022) 897–906, https://doi.org/10.1515/med-2022-0480.
[34] H. Rakhshandeh, A. Ghorbanzadeh, S.S. Negah, M. Akaberi, R. Rashidi, F. Forouzanfar, Pain-relieving effects of lawsonia inermis on neuropathic pain induced by chronic constriction injury, Metab. Brain Dis. 36 (2021) 1709–1716, https://doi.org/10.1007/s11011-021-00773-w.
[35] H. Rakhshandeh, A.M. Pourbagher-Shahri, M. Hasanpour, M. Iranshahi, F. Forouzanfar, Effects of capparis spinosa extract on the neuropathic pain induced by chronic constriction injury in rats, Metab. Brain Dis. 37 (2022) 2839–2852, https://doi.org/10.1007/s11011-022-01094-2.